Physica B: Condensed Matter 531 (2018) 16–20

Contents lists available at ScienceDirect

Physica B: Condensed Matter

journal homepage: www.elsevier.com/locate/physb

# Lattice dynamic properties of $Rh_2XAl$ (X=Fe and Y) alloys

Selgin Al [a,*], Nihat Arikan [b], Süleyman Demir [b], Ahmet Iyigör [c]

[a] Department of Physics, Faculty of Arts and Sciences, Ahi Evran University, Kırşehir, Turkey
[b] Department of Mathematics and Science, Education Faculty, Ahi Evran University, Kırşehir, Turkey
[c] Ahi Evran University, Central Research Lab, 40100 Kırşehir, Turkey

ARTICLE INFO

*Keywords:*
First-principle
DFT
Electronic structure
Phonon
Elastic constant

ABSTRACT

The electronic band structure, elastic and vibrational spectra of $Rh_2FeAl$ and $Rh_2YAl$ alloys were computed in detail by employing an *ab-initio* pseudopotential method and a linear-response technique based on the density-functional theory (DFT) scheme within a generalized gradient approximation (GGA). Computed lattice constants, bulk modulus and elastic constants were compared. $Rh_2YAl$ exhibited higher ability to resist volume change than $Rh_2FeAl$. The elastic constants, shear modulus, Young modulus, Poisson's ratio, B/G ratio electronic band structure, total and partial density of states, and total magnetic moment of alloys were also presented. $Rh_2FeAl$ showed spin up and spin down states whereas $Rh_2YAl$ showed none due to being non-magnetic. The calculated total densities of states for both materials suggest that both alloys are metallic in nature. Full phonon spectra of $Rh_2FeAl$ and $Rh_2YA1$ alloys in the $L2_1$ phase were collected using the *ab-initio* linear response method. The obtained phonon frequencies were in the positive region indicating that both alloys are dynamically stable.

## 1. Introduction

Heusler alloys have been great of interest with more than 1500 representatives due to their ferromagnetic properties and being novel alloys for energy applications [1,2]. First member of this family with a composition of $Cu_2MnAl$ was discovered by a German engineer Fritz Heusler [3]. This ternary alloy was unique since none of its constituent element is ferromagnetic by itself. These alloys with XYZ formula with an $C1_b$ structure belong to half-Heusler family while $X_2YZ$ alloys with an $L2_1$ structure belong to full- Heuslar family where X and Y are transition metals and Z is usually a member of group III to V [4]. The Heusler family exhibit different kinds of properties such as optical [5], magnetocaloric [6], structural [7], unique Curie temperatures [8] which are making them suitable for magnetic tunnel junctions, spintronic and thermoelectric applications [9].

The atomic order of Heusler alloys strongly affects their properties, even a small atomic disorder in the lattice site distributions can create a big difference in their electronic structure and hence their magnetic and transport properties [10–12]. Although, great number of alloys has been fabricated and studied with different compositions, it is not possible to synthesize all possible compositions. Thus, computational methods (quantum mechanical) are suitable tools in order to reveal the best compositions and its properties. The formation enthalpies [4], magnetic properties [13], and structural stabilities [14] of some full-Heusler alloys have been studied experimentally so far.

From this point of view, a number of Heusler alloys' formation enthalpies and electronic structures have been calculated using first principle calculations by Gilleßen et al. [15]. Their results suggested that among 810 Heusler alloys, only 12% of them is experimentally possible to synthesize. Another calculation has been done by Watson et al. [16] in order to predict the formation enthalpies of about 50 $X_2YAl$ alloys with $BiF_3$ phase, one of them was being $Rh_2YAl$. The electronic structure of $Rh_2YAl$ was investigated by Weinert et al. [17]. The standard formation enthalpy of $Rh_2YAl$ was also measured by Yin et al. [4] using high temperature direct reaction calorimetry. Even tough, considerable afford has been made in order to investigate possible combinations of these alloys, less attempt has been made to reveal these possible combinations' magnetic, structural, electronic and phonon properties theoretically. Revealing various properties such as phase transitions, thermodynamic stability, transport and thermal will allow one to employ these alloys in suitable applications without running series of experiments. For instance, full phonon-dispersion curves are necessary for a microscopic understanding of the lattice dynamics which then will play an important role in stability. Therefore, this study aims to investigate two possible combinations ($Rh_2FeAl$ and $Rh_2YAl$) in terms of electronic, structural, dynamic and magnetic properties by applying a computational method namely; density

* Corresponding author.
*E-mail address:* selgin.al@ahievran.edu.tr (S. Al).

https://doi.org/10.1016/j.physb.2017.12.020
Received 17 November 2017; Accepted 6 December 2017
Available online 7 December 2017

functional theory within the generalized gradient approximation (GGA). The results of this study will present a full description of these alloys.

## 2. Calculation method

All the calculations were done through a program package "Quantum-ESPRESSO" software [18]. The program consists of the density functional theory and plane-wave basis set. The correlation potential was computed using Perdew-Burke-Ernzerhof (PBE) approximation [19]. The interaction between electron and ion was given by the ultrasoft Vanderbilt pseudopotential [20]. 40 Ry cut off energy was used in all calculations while a 10 × 10 × 10 k-point mesh was used in Brillouin-zone integrations. The smearing technique was employed with a smearing parameter being 0.02 Ry for the integration below Fermi surface [21]. Following finding the solutions of Kohn-Sham equations, the lattice dynamic properties were computed within the density functional perturbation theory [22,23]. The phonon dispersion calculations were carried out on a 4 × 4 × 4 q-point mesh in order to get eight dynamic matrices and density of states. Fourier deconvolution was applied on this mesh for evaluation of matrices. The specific heats of alloys at a constant volume were computed using the quasi harmonic approximation (QHA) [24].

One way of calculating elastic constants is to compute the total energy using volume-conserving approach that breaks the cubic symmetry. Bulk modulus, $B$, $C_{44}$ and shear modulus, $C' = (C_{11}- C_{12})/2$, were computed using hydrostatic pressure, $e = (\delta,\delta,\delta,0,0,0)$, tri-axial shear strain, $e = (0, 0, 0,\delta,\delta,\delta)$, and volume-conserving orthorhombic strain, $e = (\delta,\delta, (1+\delta)^{-2}\text{-}1, 0, 0, 0)$ [25]. The strain ($\delta$) was taken as 0.02 for 21 sets of calculations $\left(\frac{\Delta E}{V}\right)$. Then, the bulk modulus was obtained as follows;

$$\frac{\Delta E}{V} = \frac{9}{2}B\delta^2 \tag{1}$$

where $V$ expresses the lattice cell volume before strain, $\Delta E$ expresses energy change due to strain and is represented by a vector; $e = (e_1,e_2, e_3, e_4,e_5,e_6)$. The relationship between energy change and shear modules, $C'$, can be given as;

$$\frac{\Delta E}{V} = 6C'\delta^2 + 0\delta^3 \tag{2}$$

$C_{11} = (3B + 4C')/3$ and $C_{12} = (3B - 2C')/3$ are obtained from Equation (2). $C_{44}$ is computed from the equation below:

$$\frac{\Delta E}{V} = \frac{3}{2}C_{44}\delta^2 \tag{3}$$

The detailed explanations for calculation of elastic constants $(C_{11}, C_{12}, C_{44})$ are given in Arıkan et al. [26] and Uğur et al. [27].

The hardness is given as the ability to resist to elastic deformation which can be defined by bulk modulus or shear modulus. For a cubic structure the shear modulus, $G$, can be computed from the following equations where $G_V$ is Voigt modulus and $G_R$ is Reuss modulus;

$$G_V = \frac{C_{11} - C_{12} + 3C_{44}}{5} \tag{4}$$

$$G_R = \frac{5(C_{11} - C_{12})C_{44}}{3(C_{11} - C_{12}) + 4C_{44}} \tag{5}$$

$$G = \frac{G_V + G_R}{2} \tag{6}$$

The relationship between Young modulus ($E$) and bulk-shear modulus is given by the equation below;

$$E = \frac{9BG}{3B + G} \tag{7}$$

The Poisson ratio ($\sigma$) which defines the change in volume during uniaxial distortion is given as follows;

$$\sigma = \frac{1}{2}\left(1 - \frac{E}{3B}\right) \tag{8}$$

## 3. Results

### 3.1. Structural properties

The cubic structures of $Rh_2FeAl$ and $Rh_2YAl$ alloys with the space group of Fm−3m (#225) where Rh atoms were positioned at 8c (0.25, 0.25, 0.25), Fe (Y) at 4b (0.5, 0.5, 0.5) and Al at 4a (0, 0, 0) were established in $L2_1$ phase as shown in Fig. 1. The total energy as a function of unit cell volume around the equilibrium cell volume was computed in $L2_1$ phase. Subsequently, the computed total energies were fitted Murnaghan equation [28] in order to obtain the properties given in Table 1. The lattice constant of $Rh_2YAl$ alloy with Fm−3m space group was obtained by Watson et al. [16] using full-potential linearized augmented Slater-type orbital method in literature which exhibits a clear good agreement with the lattice constant calculated in this study. Furthermore, the lattice constants obtained in this study fulfil $(a \propto 1/B)$ relationship as can be seen from Table 1.

### 3.2. Magnetic and electronic properties

The total magnetic moment of Heusler alloys exhibit Slater-Pauling behaviour (SP). According to SP, Heusler alloys fulfil the following rule, $M_t = (Z_t - 24)\mu_B$, where $Z_t$ represents the total number of valence electrons per unit cell [29]. In other words, $Z_t$ is the sum of spin up and

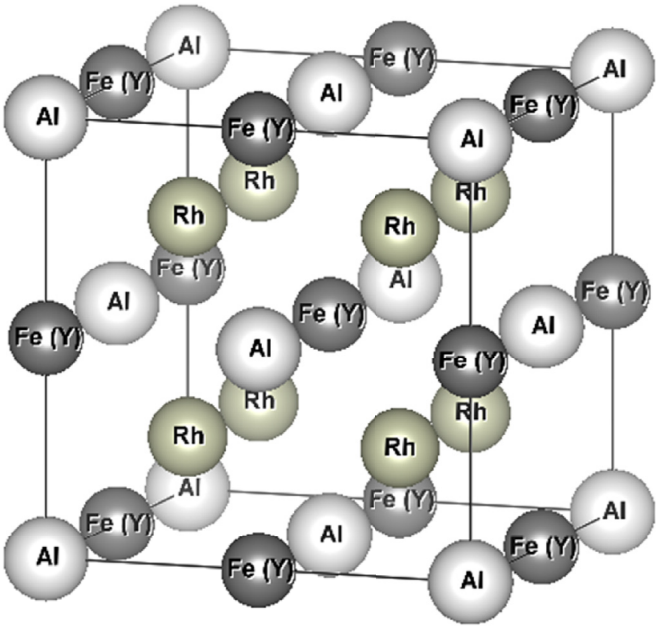


**Fig. 1.** The crystal structure of $Rh_2FeAl$ and $Rh_2YAl$ alloys in the $L2_1$ phase.

**Table 1**
The calculated lattice constants ($a_0$), bulk modulus ($B$) and total magnetic moment of $Rh_2FeAl$ and $Rh_2YAl$ alloys.

| Alloys | Ref. | $a_0$ | B | Mt ($\mu_B$) |
|---|---|---|---|---|
| $Rh_2FeAl$ | This work | 6.012 | 198.164 | 4.80 |
| | [15] | – | – | 4.26 |
| $Rh_2YAl$ | This work | 6.347 | 175.583 | 0 |
| | [16] | 6.347 | – | 0 |

spin down electrons ($Z_t = N\uparrow + N\downarrow$). The electronic configuration of $Rh_2FeAl$ and $Rh_2YAl$ full-Heusler alloys for the chosen pseudo potentials are; for Rh atom [Kr] $4d^8\ 5s^1$, for Fe atom [Ar] $3d^7\ 4s^1$, for Y atom [Kr] $4d^1\ 5s^2$ and for Al atom [Ne] $3s^2\ 3p^1$, respectively. Therefore, it is expected that the total magnetic moment (based on SP) would be around 5 $\mu_B$ and 0 $\mu_B$ for $Rh_2FeAl$ and $Rh_2YAl$ alloys. The total magnetic moment calculation for $Rh_2FeAl$ resulted in 4.80 $\mu_B$ whereas 0 $\mu_B$ was found for $Rh_2YAl$, showing a good agreement with SP rule. The results suggest that $Rh_2YAl$ is a non-magnetic material which overlaps the results of Gilleßen et al. [15] findings. Figs. 2 and 3 demonstrate the electronic band structure and density of states for the alloys. As can be seen from the figures that $Rh_2FeAl$ has spin up and spin down states, however, $Rh_2YAl$ does not have this anti-symmetric dispersion due to being non-magnetic. Therefore, electronic band structure and density of states for $Rh_2FeAl$ alloy were shown for spin up and spin down cases whereas no spin orientation was taken into account for $Rh_2YAl$ alloy. It is clear from Fig. 2 that these alloys are metallic in nature since Fermi level (which was set to 0 eV) is cut by valence and conduction band and also there is no gap at the Fermi level.

Fig. 3 displays total and partial density of states for the alloys at the Fermi level which are $n(E_F\uparrow) = 0.53$ states/eV CELL and $n(E_F\downarrow) = 2.30$ states/eV CELL for $Rh_2FeAl$ and $n(E_F) = 1.52$ states/eV CELL for $Rh_2YAl$ per unit formula. For $Rh_2FeAl$ alloy, spin down direction has higher involvement in the conduction properties. The contribution to the band for $Rh_2FeAl$ comes from Al-*3p* and Rh-*4d* states (spin up) and Fe-*3d* and Rh-*4d* states (spin down) above the Fermi level. $Rh_2YAl$ gets the main contribution from Rh-*4d*, Y-*4d* and Al-*3p* states. As Fig. 3 illustrates, for $Rh_2FeAl$ alloy, the structure below −1 eV originates from Rh-*4d* states while above −1 eV is due to Fe-*3d* states. On the other hand, for $Rh_2YAl$ alloy, the structure is derived from Rh-*4d* states below 1.5 eV and Y-*4d* states above 1.5 eV. These findings are in a good agreement with Gilleßen et al. [15] and Watson et al. [16].

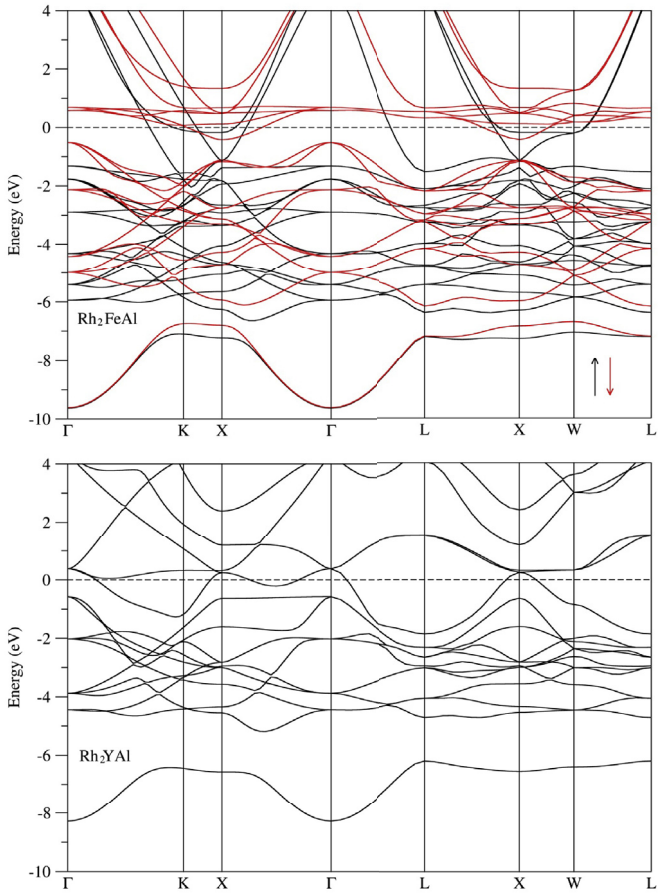


**Fig. 2.** The electronic band structure of $Rh_2FeAl$ and $Rh_2YAl$ alloys.

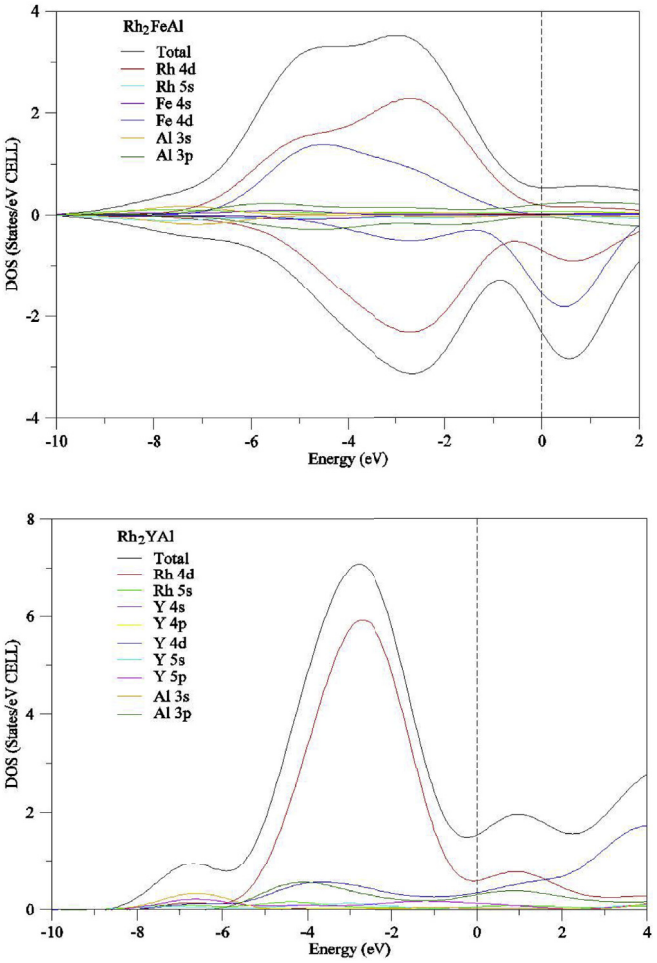


**Fig. 3.** The electronic total and partial density of states of $Rh_2FeAl$ and $Rh_2YAl$ alloys.

### 3.3. Elastic properties

Elastic constants provide information about mechanical and structural stability of a material and also it relates both properties with each other [30]. The cubic crystals with Fm−3m space group and $L2_1$ phase have three different elastic constants, namely; $C_{11}$, $C_{12}$ and $C_{44}$. In order to calculate elastic constants ($C_{ij}$), the change in total energy was obtained by applying small strains to the lattice. Then, the formulas explained in the calculation method section were used to obtain elastic constants. The elastic constants of $Rh_2FeAl$ and $Rh_2YAl$ alloys are presented in Table 2. The Born stability condition [31] of elastic constants for these alloys in $L2_1$ cubic phase can be expressed as follows;

$$C_{11} > 0,\ (C_{11} / C_{12} > 1),\ (C_{11}^2 - C_{12}^2) \text{ and } (C_{11} + 2C_{12}) > 0 \quad (9)$$

As Table 2 shows clearly that this condition is satisfied by these alloys. Thus, it can be said that $Rh_2FeAl$ and $Rh_2YAl$ full-Heusler alloys are mechanically stable in $L2_1$ phase.

Additionally, Table 2 exhibits that $C_{11}$ has the highest value for both $Rh_2YAl$ and $Rh_2FeAl$. The value of $C_{11}$ provides information about compressive resistance along x-axis [32]. Hence, both alloys illustrate incompressibility in the x direction. Also, by using computed elastic

**Table 2**
The calculated elastic constants (*Cij*) of $Rh_2FeAl$ and $Rh_2YAl$ alloys.

| Alloys | Ref. | $C_{11}$ | $C_{12}$ | $C_{44}$ |
|---|---|---|---|---|
| $Rh_2FeAl$ | This work | 258.022 | 168.235 | 127.262 |
| $Rh_2YAl$ | This work | 274.728 | 126.010 | 85.651 |

**Table 3**
The calculated bulk modulus ($B$), shear modulus ($G$, $G_v$ and $G_R$), $B/G$ ratio, Young modulus ($E$), and Poisson ratio ($\sigma$) of $Rh_2FeAl$ and $Rh_2YAl$ alloys.

| Alloys | Ref. | $B$ | $G$ | $G_v$ | $G_R$ | $B/G$ | $E$ | $\sigma$ |
|---|---|---|---|---|---|---|---|---|
| $Rh_2FeAl$ | This work | 198.164 | 83.855 | 94.314 | 73.396 | 2.36 | 220.468 | 0.31 |
| $Rh_2YAl$ | This work | 175.583 | 80.940 | 81.134 | 80.746 | 2.17 | 210.479 | 0.30 |

constants, bulk modulus, shear and Young modulus, Poisson's ration and B/G ratio were obtained and presented in Table 3. By comparing bulk and shear modulus, it can be seen that bulk modulus is higher that shear modulus for both alloys, suggesting that both alloys can resist the volume change under pressure. By comparing bulk modulus of two alloys, it can be said that $Rh_2YAl$ has higher ability to resist volume change than $Rh_2FeAl$.

According to Pugh criteria, if the $B/G$ ratio is higher than 1.75, the materials are ductile, if not, the materials are brittle [20]. The $B/G$ ratio for $Rh_2FeAl$ is 2.36 and 2.17 for $Rh_2YAl$, both of them higher than 1.75. Therefore, both alloys have ductile nature. The stiffness of the alloys were analysed by comparing Young modulus. Higher Young modulus indicates better stiffness, thus $Rh_2FeAl$ is the stiffest alloy in this study. As can be seen from Table 3 that bulk modulus, Young modulus and shear modulus have the same tendencies, all of them are higher for $Rh_2FeAl$.

It is also possible to obtain information about electronic properties via elastic constants. According to Pugh criteria, if the Poisson's ratio is around 0.1, the material has covalent bonding, if it is around 0.25, the material has ionic bonding [20]. Based on the Poisson's ratios presented in Table 3, both alloys have ionic-metallic interaction.

### 3.4. Phonon properties

$Rh_2FeAl$ and $Rh_2YAl$ full-Heusler alloys in $L2_1$ phase have four atoms per primitive cubic unit cell and twelve phonon modes (due to 3N degrees of freedom) with three of them being acoustical, the rest is optical. Fig. 4 demonstrates density of states and phonon dispersion curves for these alloys. The phonon modes reduced from twelve to eight between X-Γ-L high symmetry directions. The dispersion curves are in the positive phonon frequency range. Thus, both alloys are dynamically stable. The optic phonon modes of these alloys have band gaps, which is 1.55 THz for $Rh_2FeAl$ and 0.59 THz for $Rh_2YAl$. The partial density of states indicates that the frequencies above the band gap are owing to Al atoms since the atomic weight of Al is less than other atoms. For $Rh_2YAl$ alloy, the transverse acoustic (TA) gets softener between Γ-K and X-Γ high symmetry directions. Acoustical phonon frequencies mostly come from Rh atoms for $Rh_2FeAl$ whereas they are due to vibrations of Rh and Y atoms for $Rh_2YAl$. In the centre of Brillioun zone, the optic phonons were computed as 6.118, 6.593 and 9.098 THz for $Rh_2FeAl$ and 5.122, 6.461 and 8.072 THz for $Rh_2YAl$. It can be said that in those frequency ranges full-Heusler

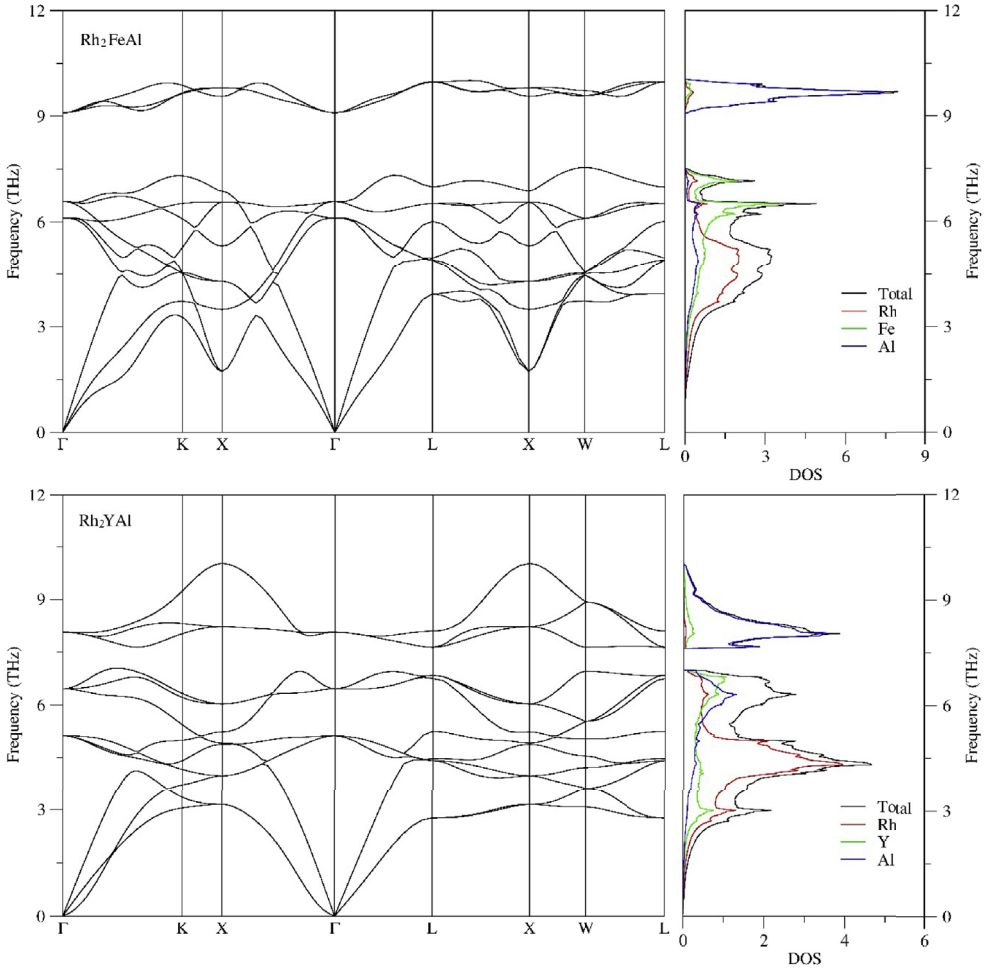


**Fig. 4.** Full phonon spectra and projected density of states of $Rh_2FeAl$ and $Rh_2YAl$ alloys.

alloys have Raman and IR active states. Unfortunately, theoretical or experimental phonon spectrums of $Rh_2FeAl$ and $Rh_2YAl$ alloys are not available in literature for further comparison. Thus, we hope that this will add new data to literature for future investigations.

## 4. Conclusions

The electronic, magnetic, elastic and phonon properties of $Rh_2FeAl$ and $Rh_2YAl$ alloys with Fm−3m (#225) space group in $L2_1$ phase were computed using density functional theory. Firstly, the lattice constants of the alloys in $L2_1$ phase were obtained. Those values were compared with the available data and found a good agreement for $Rh_2YAl$. Furthermore, the result indicated an inverse correlation between bulk modulus and lattice constants of two alloys. $Rh_2FeAl$ was found to be a magnetic material whereas $Rh_2YAl$ showed a non-magnetic nature. The total magnetic moments of two alloys were similar to the values obtained from SP. The electronic structure analyses revealed that both alloys have metallic character. The elastic properties of them suggest that these alloys in $L2_1$ phase are mechanically stable. Additionally, bulk, shear and Young modulus of alloys, *B/G* and Poisson's ratio were analysed. According to *B/G* ratio, these alloys are ductile. Young modulus suggested that they are stiff. Bulk and shear modulus revealed their incompressible nature. Poisson's ratio showed their ionic-metallic character. Unfortunately, there is no available data for comparison of phonon and elastic properties. However, their phonon frequencies exhibit that these alloys are dynamically stable.

## References


[1] M. Yin, Thermodynamic Properties and Phase Equilibria of Selected Heusler Compounds, Illinois Institute of Technology, Ann Arbor, 2015, p. 257.
[2] T. Graf, C. Felser, S.S.P. Parkin, Simple rules for the understanding of Heusler compounds, Prog. Solid State Chem. 39 (1) (2011) 1–50.
[3] F. Heusler, V. Dtsch, Mangan-aluminium-kupferlegierungen, Phys. Ges. 12 (1903) 219.
[4] M. Yin, P. Nash, Standard enthalpies of formation of selected $Ru_2YZ$ Heusler compounds, J. Alloys Compd. 634 (2015) 70–74.
[5] P.G.V. Engen, et al., PtMnSb, a material with very high magneto-optical Kerr effect, Appl. Phys. Lett. 42 (2) (1983) 202–204.
[6] T. Krenke, et al., Inverse magnetocaloric effect in ferromagnetic Ni-Mn-Sn alloys, Nat. Mater 4 (6) (2005) 450–454.
[7] R. Kainuma, et al., Magnetic-field-induced shape recovery by reverse phase transformation, Nature 439 (7079) (2006) 957–960.
[8] W. Sabine, et al., Structural properties of the quaternary Heusler alloy Co 2 Cr 1− x Fe x Al, J. Phys. D Appl. Phys. 40 (6) (2007) 1524.
[9] W. Wang, et al., Coherent tunneling and giant tunneling magnetoresistance in $Co_2FeAl$ - MgO - CoFe magnetic tunneling junctions, Phys. Rev. B 81 (14) (2010), 140402.
[10] S. Picozzi, A. Continenza, A.J. Freeman, Role of structural defects on the half-metallic character of $Co_2MnGe$ and $Co_2MnSi$ Heusler alloys, Phys. Rev. B 69 (9) (2004), 094423.
[11] Y. Miura, K. Nagao, M. Shirai, Atomic disorder effects on half-metallicity of the full-Heusler alloys $Co_2Cr_{1-x}Fe_x$: a first-principles study, Phys. Rev. B 69 (14) (2004), 144413.
[12] K. Hem Chandra, et al., Electronic structure, magnetism and disorder in the Heusler compound Co 2 TiSn, J. Phys. D Appl. Phys. 40 (6) (2007) 1587.
[13] H. Yako, et al., Magnetic properties of Mn-rich Rh2Mn1+xSn1−x Heusler alloys, Phys. B Condens. Matter 407 (3) (2012) 311–315.
[14] J.C. Suits, Structural instability in new magnetic heusler compounds, Solid State Commun. 18 (3) (1976) 423–425.
[15] M. Gilleßen, R. Dronskowski, A combinatorial study of full Heusler alloys by first-principles computational methods, J. Comput. Chem. 30 (8) (2009) 1290–1299.
[16] R.E. Watson, M. Weinert, M. Alatalo, Ternary transition-metal aluminide alloy formation: the $BiF_3$ structure, Phys. Rev. B 57 (19) (1998) 12134–12139.
[17] M. Weinert, R.E. Watson, Hybridization-induced band gaps in transition-metal aluminides, Phys. Rev. B 58 (15) (1998) 9732–9740.
[18] S. Baroni, et al., Quantum ESPRESSO: open-source package for research in electronic structure, simulation, and optimization, Code available from: http://Quantum-espresso.org, 2005.
[19] J.P. Perdew, K. Burke, M. Ernzerhof, Generalized gradient approximation made simple, Phys. Rev. Lett. 77 (18) (1996) 3865–3868.
[20] S.F. Pugh, XCII. Relations between the elastic moduli and the plastic properties of polycrystalline pure metals, Philosophical Mag. J. Sci. 45 (367) (1954) 823–843.
[21] M. Methfessel, A. Paxton, High-precision sampling for Brillouin-zone integration in metals, Phys. Rev. B 40 (6) (1989) 3616.
[22] S. Baroni, et al., Phonons and related crystal properties from density-functional perturbation theory, Rev. Mod. Phys. 73 (2) (2001) 515–562.
[23] S. Baroni, P. Giannozzi, A. Testa, Green's-function approach to linear response in solids, Phys. Rev. Lett. 58 (18) (1987) 1861–1864.
[24] S. Baroni, P. Giannozzi, E. Isaev, Density-functional perturbation theory for quasi-harmonic calculations, Rev. Mineralogy Geochem. 71 (1) (2010) 39.
[25] S.Q. Wang, H.Q. Ye, First-principles study on elastic properties and phase stability of III–V compounds, Phys. Status Solidi (b) 240 (1) (2003) 45–54.
[26] N. Arıkan, et al., Structural, elastic, electronic and phonon properties of scandium-based compounds ScX3 (X = Ir, Pd, Pt and Rh): an ab initio study, Comput. Mater. Sci. 79 (2013) 703–709.
[27] Ş. Uğur, et al., Structural, electronic and vibrational properties of ordered intermetallic alloys CoZ (Z = Al, Be, Sc and Zr) from first-principles total-energy calculations, Philos. Mag. 93 (24) (2013) 3260–3277.
[28] F.D. Murnaghan, The compressibility of media under extreme pressures, Proc. Natl. Acad. Sci. U. S. A. 30 (9) (1944) 244–247.
[29] I. Galanakis, M. Ph, P.H. Dederichs, Electronic structure and Slater–Pauling behaviour in half-metallic Heusler alloys calculated from first principles, J. Phys. D Appl. Phys. 39 (5) (2006) 765.
[30] A. İyigör, Ş. Uğur, Elastic and phonon properties of quaternary Heusler alloys CoFeCrZ (Z = Al, Si, Ga and Ge) from density functional theory, Philos. Mag. Lett. 94 (11) (2014) 708–715.
[31] M. Born, K. Huang, Theory of Crystal Lattices, Clarendon, Oxford, 1956.
[32] M. Wang, et al., Structural, elastic and thermodynamic properties of A15-type compounds V3X (X= Ir, Pt and Au) from first-principles calculations, Mod. Phys. Lett. B (2016), 1650414.